OPEN ACCESS Pakistan Journal of Biological Sciences

ISSN 1028-8880
DOI: 10.3923/pjbs.2021.953.970

Research Article
Characterization of Biofilm Producer Nanobacteria Isolated from Kidney Stones of Some Egyptian Patients

[1]Nora Fayez Hassan, [2]Mohamed Khaled Ibrahim, [1]Seham Yousef El Tablawy and [1]Hala Abd Allah Farrag

[1]National Center for Radiation Research and Technology (NCRRT), Department of Drug Radiation Research, Egyptian Atomic Energy Authority, Egypt
[2]Department of Microbiology, Faculty of Science, Ain shams University, Egypt

Abstract

Background and Objective: Nanobacteria (NB) appear to contribute to many calcifying diseases including kidney stones which represent a common problem with inadequate prevention exist. NB framing itself with a mineral coat that assists as a primary defence shield against the immune system, antibiotics. This study aims to collect and detect nanobes from different kidney stones from patients with active urolithiasis then investigated the anti-nano-bacterial activity of some antibiotics alone or in combination with extracts of irradiated herbs of certain medicinal plants which will represent a new approach to therapy for patients with kidney stones. **Materials and Methods:** Total of 32 nanobes were isolated from 54 kidney stones. Fourier Transforms Infrared Spectroscopy (FTIR) revealed that calcium and phosphate are the main components of stones. Scanning Electron Microscopy (SEM) with Energy-dispersive X-ray spectroscopy (EDX) and Transmission Electron Microscope (TEM), showed that nanobes were Gram-ve cocci with size ranged from (375:600 nm). The biofilm production ability of nanobes was estimated qualitatively and quantitatively. **Results:** The results revealed that all were strong biofilm producers. Further, the antibiotic susceptibility test indicates their resistance towards most of the tested antibiotics. Molecular identification of the strong biofilm producer isolates by ribosomal ribonucleic acid (rRNA) revealed that it is indicated by 85.37% to *Bartonella apis* strain PEB0122. **Conclusion:** The findings of the current study evidenced that combination treatment between Doxycycline (DO) and water extract of khella exhibited a significant reduction in biofilm formation ability of the strongest producers nanobes. Therefore, this treatment can play a role in enhancing public health, especially with patients who suffer from recurrent kidney stone formation.

Key words: Nanobacteria (NB), scanning electron microscopy (SEM), transmission electron microscope (TEM), medicinal plant extracts, γ-irradiation, coccoid, biofilm formation, ribosomal ribonucleic

Citation: Hassan, N.F., M.K. Ibrahim, S. Yousef El Tablawy and H.A.A. Farrag, 2021. Characterization of biofilm producer nanobacteria isolated from kidney stones of some Egyptian patients. Pak. J. Biol. Sci., 24: 953-970.

Corresponding Author: Seham El-Tablawy, National Center for Radiation Research and Technology (NCRRT), Department of Drug Radiation Research, Egyptian Atomic Energy Authority, Egypt

Competing Interest: The authors have declared that no competing interest exists.

Data Availability: All relevant data are within the paper and its supporting information files.

INTRODUCTION

Nanobacteria (NB) are the smallest cell-walled bacteria that have been founded in human and cow blood, as well as in commercial cell culture serum. Their diameter ranged from 100-600 nm thus can pass through sterilization filters[1]. They have coccoid, coccobacillus, or bacillar form. They are Gram-negative and can be stained by DNA-specific dyes[2]. Biological structures of nanobacteria composed of C, O and N. According to the 16S rRNA gene sequence, NB falls within the α-2 subgroup of Proteobacteria, which also comprise human pathogens as *Brucellaceae* and *Bartonella* species[3]. They are self-replicating by binary fission and fragmentation. They grow greatest under anaerobic conditions. Their doubling time is three days and their metabolism is 10,000 times slower than in *Escherichia coli*[2].

Nanobacteria have unusual properties, making their detection hard with standard microbiological methods. An investigation by SEM revealed similar coccoid shapes with a diameter of 100-600 nm, their rough surfaces with a distinct cell wall and a capsule shielded with a hairy apatite layer had been seen in TEM micrographs[1]. Its replication can be measured by optical density at 650 nm. Also, it has been shown by other specific methods, such as ELISA[4].

NB appear to show a correlation with diverse calcification-related health problems including arterial heart disease, Alzheimer's disease, polycystic kidney disease, gall stones and gallbladder inflammation, cancer and prostatitis[5]. Nanobacteria can also cause kidney stones and its antigen has been stated in 97% of human kidney stones. These bacteria framing themselves with a mineral coat (biofilm) and can serve as nidi for the genesis of renal calculi[6,7]. The phyto-preparations of medicinal plants have acquired special interest in recent decades as alternative products that could resolve problems associated with the appearance of strains of microorganisms with reduced susceptibility to antibiotics. WHO documented that approximately 80% of the world populations still rely mainly on herbal remedies[8].

Hence, this study was conducted to investigate the occurrence of NB in kidney stones collected from Egyptian patients with urolithiasis based on a morphological mark through different techniques. In addition, water and ethanolic extracts of different medicinal plants used in folk medicine for kidney stones treatment were tested on the growth of NB and biofilm formation ability.

MATERIALS AND METHODS

Study area: The study was carried out at the Medical Microbiology Laboratory, National Center for Radiation Research and Technology (NCRRT), Department of Drug Radiation Research, Egyptian Atomic Energy Authority, Egypt from March, 2018-2020).

Collection of kidney stones and their preparation for different investigations: Fifty-four human kidney stones were collected from 54 male and female patients with active Urolithiasis from different medical labs, Cairo, Egypt. These collected stones were washed with sterile distilled water, dried, pulverized and stored at 4°C in plastic vials. Stone samples were employed for compositional stone analysis and isolation of NB.

Chemical analysis of the collected stones using Fourier Transforms Infrared Spectroscopy (FTIR): The powdered stone samples were diluted with potassium bromide in a ratio of 1:100 and dried at room temperature; they were compacted for forming discs. They were later exposed to FT-IR spectroscopy measurements using JASCO FT-IR-3600 spectrometers (Easton, USA) located in NCRRT, in a wavenumber region of 500-3500 cm^{-1}. Data were collected at a resolution of 4 cm^{-1}.

Isolation and detection of nanobacteria

Isolation of nanobacteria: To isolate nanobacteria, 0.15-0.5 g of 54 pulverized stones were manually demineralized by incubation with 1 N HCl for 10 min with continuous stirring at room temperature and neutralized by the addition of 1 N NaOH for 10 min with constant stirring. Then centrifuged using a cooling centrifuge (Werk Nr., Germany) at 14, 000 g for 15 min, the pellet was suspended in Dulbecco's modified Eagle medium (DMEM) (sigma)and sieved through a 0.45-mm membrane filter. Finally, 1 mL of the suspended pellet was inoculated into 25 mL sterile Erlenmeyer flasks containing 15 mL of standard DMEM and incubated at 37°C in humidified anaerobic condition for 4 weeks. Subculture was carried out every 14 days and the presence of nanobacteria was observed using macroscopic and microscopic techniques, as well as spectrophotometer and SEM investigations.

Nano-bacterial isolates were preserved in 30% glycerol stock at 4°C for further investigations. To investigate the possibility of the presence of any contaminants during the growth period, the filtered solution was cultured in the Luria-Bertani medium (TM Media) for one weak at 37°C.

Detection of nanobacteria

Detection of nano-bacterial growth by spectrophotometer: Nanobacteria replication was evaluated during time intervals using U.V. visible spectrophotometer (T60 U-PG instrument limited) at Optical Density (OD) 650 nm wavelengths. Negative nano-bacterial detection was confirmed by the absence of any detectable rise in OD throughout the test period (28 days)[9]. While samples with positive growth were over confirmed by SEM and TEM.

Macroscopic and microscopic detection of nanobacteria: Nano-bacterial growth was observed macroscopically by the naked eye during incubation periods. Flask with medium only was used as control. For microscopic detection, nano-bacterial culture was centrifuged at 20.000 g for 30 min; the pellet was washed by phosphate buffer pH (7.2), then it was stained by Gram staining technique and examined by Light Microscope (LM) at oil lens (100/1.25).

Urease production test: Urease test is applied to identify those organisms that are capable of hydrolyzing urea to produce ammonia and carbon dioxide according to Christensen[10].

Detection of nanobacteria by SEM with EDX and TEM: The surface morphology and elemental analysis of nanobacteria were investigated using SEM supported by the EDX unit and TEM.

The surface morphology was studied by SEM as follow: 30-day old nano-bacterial culture was harvested by centrifugation at 20,000 g for 30 min at 4°C. The bacterial pellet was washed in a phosphate-buffered solution (pH 7.2) then was dehydrated in absolute alcohol and air-dried overnight.

Finally, the sample was investigated using a JEOL-JEM 5400 scanning electron microscope, JEOL, JFC- 1100E ION SPUTTERING DEVICE at NCRRT[11]. EDX spectra recorded on BRUKER Nano GmbH D-12489, 410-M (Berlin-Germany) was used to anatomize elemental structure of NBs pellet from 1-month-old culture material by applying mapping technique to supply full information about the composition of a bacterial cell wall, cell membrane and internal organelles.

Examination by TEM was carried out as follows: the specimens were fixed by immersion in 1% potassium permanganate solution for 5 min at room temperature. Then they were dehydrated in ethyl alcohol, embedded in epoxy and ultra-thin sections were cut and placed on 200 mesh copper grids. The sections were stained with uranyl acetate and lead citrate and examined using a JEOL-JEM 1010 TEM at 80 kV at the Regional Center for Mycology and Biotechnology (RCMB), Al-Azhar University, Egypt[12].

Chemical analysis of the nano-bacterial shield using Fourier Transforms Infrared Spectroscopy (FTIR): The nano-bacterial pellet was washed with phosphate buffer saline three times and was analyzed as previously mentioned.

Qualitative determination of biofilm production by nano bacterial isolates[13]: The NB isolates were tested for their ability to produce biofilm. Following 4 weeks of incubation, after withdrawal of the contents, the tubes were washed twice with distilled water, then, 0.1% crystal violet was added. Biofilm production was judged to have occurred if a visible continuous stained thick film lined the inner walls of the tube. The experiments were repeated three times. The amount of stained biofilm was semi quantitated and estimated by three independent observers as strong (+++), moderate (++) and weak (+).

Quantitative determination of biofilm production by nano-bacterial isolates using ELISA method: Adherence was measured by using spectrophotometric methods defined by Christensen *et al.*[14].

Total 200 µL of nano bacterial culture with turbidity equivalent to that of a 0.5 McFarland standard was added to each well of sterile, polystyrene, flat bottom tissue culture plate (Sigma-Aldrich, Costar and the USA). In the case of control well; 200 µL of DMEM was added. Following 28 days of incubation at 37°C in humidified anaerobic condition.

The contents of tissue culture plates were gently aspirated with micropipette then washed three times with sterile phosphate buffer saline (pH 7.2) to eliminate free-floating planktonic bacteria. Slime and adherent organisms were fixed by incubating them for 1 hr at 60°C[15] and staining them with Hacker crystal violet (0.1% w/v) for 5 min. After washing with water to remove the extra stain, the plates were dried for 30 min at 37°C and Optical Densities (ODs) of the stained adherent biofilm were read with Micro ELISA Auto Reader at wavelength 630 nm. Adherence measurements were performed in triplicate and the values were averaged. The isolates were categorized based on ODs as weak, moderate or highly adhered according to Vasanthi *et al.*[16].

Identification of nanobacteria by 16S rRNA and phylogenetic analysis: To study the molecular identification of the most drug-resistant and potent biofilm producer isolates, the nano-bacterial whole genome was extracted by extraction kits from Zymo Research as follow: In a microcentrifuge tube containing 200 µL of nano-bacterial culture, add 95 µL water, 95 µL solid tissue buffer (blue) and 10 µL proteinase K. Mix thoroughly and incubate the tube at 55°C for 2 hrs. Following incubation, mix thoroughly and centrifuge at 12,000×g for 1 min then transfer the supernatant to a clean tube (300 µL), add 600 µL Genomic Binding Buffer and mix thoroughly. The mixture was transferred to a Zymo-Spin™ IIC-XL Column in a Collection Tube. Centrifuge (≥12,000×g) for 1 min. Add 400 µL DNA Pre-Wash Buffer and centrifuge at (12.000×g) for 1 min then add 700 µL g-DNA wash buffer and centrifuge at (12.000×g) for 1 min, empty the collection tube and add 200 µL g-DNA wash buffer and centrifuge at (12.000×g) for 1 min. Finally, discard the collection tube, add 30 µL elution buffer incubate for 5 min and then centrifuge again at (12.000×g) for 1 min (Sigma-Scientific Services Company).

Antibiotic susceptibility patterns of the strongest nano-bacterial biofilm producers: The most potent biofilm-producing nano-bacterial isolates were subjected to antibiotics sensitivity test using 6 different antibiotics agents (Streptomycin (S), Doxycycline (DO), Cefepime (CEP), Trimethoprim/sulfamethoxazole (SXT), Penicillin G and Ciprofloxacin (CIP)) which are commonly used for the treatment of urolithiasis.

The National Committee for Clinical Laboratory Standards (NCCLS)[17] has no information on susceptibility methods of NB. So, this test was carried out spectroscopically as follows: antimicrobials were dissolved in DMEM and sterilized by membrane filtration (pore size, 0.2 µm; Millipore Corp., Bedford, Mass.) according to Hannan *et al.*[18]. Total 1 mL of each antibiotic was transferred to a tube containing 1 mL of nano-bacterial suspension with turbidity equivalent to that of a 0.5 McFarland standard (optical density at 650 nm). Another tube of NB and devoid of any drug was used as the growth control while another tube with an uninoculated medium was served as the sterility control. Tubes were incubated at 37°C in a humidified anaerobic atmosphere for a maximum of 14 days.

The effect of the tested antibiotics on the growth of different nano-bacterial isolates was monitored by reading with a spectrophotometer at wavelength 650 nm. The experiment was performed in triplicate.

Irradiation process: This test was done to evaluate the quality of the tested plants from the point of view of microbiology. The samples under study were subjected to γ-irradiation doses using Cobalt-(60 Co) 220 Gamma cell, a product of Canada Co. Ltd. locate NCRRT. The dose rate at the time of the experiment was 1.323 kGy/H.

Microbiological quality of medicinal plants: Samples of the tested medicinal plants; thistle, parsley, khella, dill, thyme, halfa bar, neem and fennel were packed (3 g) in polyethylene bags and exposed to γ-radiation doses ranged from 1-10 kGy. Each sample was suspended in a 27 mL sterile saline solution flask (0.89% $NaCl/H_2O$) containing few drops of tween 20. The flasks were shaken on a rotary shaker (200 rpm) and a decimal dilution of suspension was made.

The bacterial count was determined on a plate count agar medium containing 100 µg mL^{-1} Mycostatin at 32±1°C for 24-48 hrs according to ICMSF[19]. Fungi were counted on Sabouraud dextrose agar medium containing 10 µg mL^{-1} ox tetracycline hydrochloride and the plates were incubated at 25°C for 7 days. The experiment was performed in triplicate[20].

Preparation of water and ethanolic extracts: Water Extracts (WEs) of the tested plants were prepared according to Charchafchi *et al.*[21]. While, Ethanolic Extracts (EEs) were obtained as described by Najmadeen *et al.*[22].

Screening for the effect of the anti-nano-bacterial agent on biofilm production of nano-bacterial isolates: The adherence of nano-bacterial isolates was determined by Christensen *et al.*[14]. Testing the ability of antibiotics and medicinal plant extracts to prevent nano-bacterial adherence was designed as previously mentioned

Minimum inhibitory concentrations of some selected anti-nano-bacterial agents on biofilm production of nano-bacterial isolates: Minimum inhibitory concentrations of the most effective antimicrobials; antibiotics, WEs and EEs of medicinal plants were determined as follows: antimicrobials were dissolved in DMEM to give a final concentration of 500 mg mL^{-1} and sterilized by membrane filtration (pore size, 0.2 µm; Millipore Corp., Bedford, Mass.). Then antimicrobial dilutions were prepared just before use in sterile plastic vials at double the required concentration in DMEM to allow 1:1 dilution of the inoculum of NB in MIC tests. The NB isolates were tested against each antibiotic at concentrations ranging from 500-1.9 µg mL^{-1}. Finally, MIC determination of the most effective antibiotics and medicinal plant extracts was designed as previously mentioned.

Combination treatment between the most potent agents on biofilm production of the nano-bacterial isolates: The nano-bacterial culture was adjusted with a turbidity equivalent to that of a 0.5 McFarland standard (optical density at 650 nm). MIC_S of the choice antibiotics and medicinal plant extracts were prepared. Combination treatment between the most potent agents on biofilm production of the strongest nano-bacterial biofilm producer isolates was designed as previously mentioned.

Statistical analysis: Statistical analysis was performed using one-way analysis of variance (ANOVA) followed by post hoc Turkey's HSD (Honestly Significant Difference) test by Graph Pad Prism 5 software package. Data were presented as Mean ± SE with an acceptable level of significance of $p \leq 0.05$. The method used for the analysis of the results is that given by Milton *et al.*[23].

RESULTS

Collection of kidney stones: In this study 54 kidney stones were collected from 54 males and female's patients from different labs, Cairo, Egypt. The collected stones appeared in different sizes and shapes.

The results in Table 1 showed that, among these collected stones, 9 (16.67%) were from females and 45 (83.33%) were from males, with variable ages between 30-60 years.

Chemical analysis of the collected stones using Fourier Transforms Infrared Spectroscopy (FTIR): The results presented in Table 2 revealed that out of 54 samples, 24 (44.44%) samples were found to be a mixture of (COM) and (CaP). The important five spectral bands between 3427-3047 cm^{-1} are due to pure COM and symmetric and asymmetric O-H stretch. Absorptions at 1610 and 1313 cm^{-1} may be due to the vibration of C = O and C-O of oxalate respectively.

The absorption band at 880 cm^{-1} was due to C-C stretching mode. While, the bands at 654 and 774 cm^{-1} are due to the out of plane O-H bending and C-H bending mode respectively and finally, the band at 508 cm^{-1} arises due to O-C-O in-plane bending (Fig. 1a).

While thirteen stones (24.07%) were found to be a combination of Ca P and Ca OX. The band at 3334 cm^{-1} was due to symmetric and asymmetric O-H stretch. Absorption at 1612 and 1311cm^{-1} was due to C = O, C-O groups of calcium oxalate. Regarding the bands at 1026 and 772 cm^{-1} is found to be due to P-O of PO^{-34} and asymmetric of C = O, respectively (Fig. 1b).

Whereas, 12 stones (22.22%) struvite have a characteristic infrared spectrum by the position of the band at 1114 cm^{-1}, which is due to the absorption of the PO_4 group. Also, bands between 3428-26303 cm^{-1} are due to OH-N-H stretching. The bands at 1628 and 1582 cm^{-1} were due to the vibration of the NH group. The absorbance band at 988 cm^{-1} shows the aliphatic stretching of P-O (Fig. 1c).

However, 3 stones (5.56%) were a mixture of AmU and P. Its FTIR spectrum (Fig. 1d) investigated the presence of five bands between 3007-2672 cm^{-1}, which were due to N-H stretching of heterocyclic and ammonium groups. Absorption at 1633 and 1588 cm^{-1} may be due to carbonyl of urea and conjugated carbonyl, respectively. While the band at 1271 cm^{-1} was due to O = C-H bending mode. The phosphate group usually has an absorption band in the range of 1000-1100 cm^{-1}.

Table 2 and (Fig. 1e) indicated that two stones (3.71%) out of 54 were found to be a combination of (COD and CaP). The band at 3221 cm^{-1} was due to the presence of the O-H group. The absorbance at 1636 and 1389 cm^{-1} shows the presence of C = O and C-O stretching vibrations. The presence of other bands at 759, 608 cm^{-1} are for C-H bending and 517 cm^{-1} for the O-C-O plane. PO_4 group has an absorption band at 999 cm^{-1}.

In this study, the chemical analysis of the examined stones indicated that the most predominant types of stones were COM and CaP (44.44%), followed by CaP and Ca OX (24.07%), while Mg AmP, AmU and P and COD and CaP were 22.22, 5.56 and 3.71%, respectively.

Table 1: Frequency of urolithiasis with different groups of age and sex

	No. of bacterial stone		
Age/years	Female (%)	Male (%)	Total no. (%)
30-35	3 (5.56%)	12 (22.22%)	15 (27.78%)
36-46	5 (9.26%)	18 (33.33%)	23 (42.59%)
47-60	1 (1.85%)	15 (27.78%)	16 (29.63%)
Total	9 (16.67)	45 (83.33)	54

Table 2: Prevalence of different chemical structures of kidney stones (n = 54)

Kidney stones types	Total number of stones	Prevalence (%)
Calcium oxalate monohydrates and calcium phosphate (COM and CaP)	24	44.44
calcium phosphate and calcium oxalate (CaP and Ca OX)	13	24.07
Struvite (magnesium ammonium phosphate (Mg AmP)	12	22.22
ammonium urate and phosphate (AmU and P)	3	5.56
e-calcium oxalate dehydrate and calcium phosphate (COD and CaP)	2	3.71

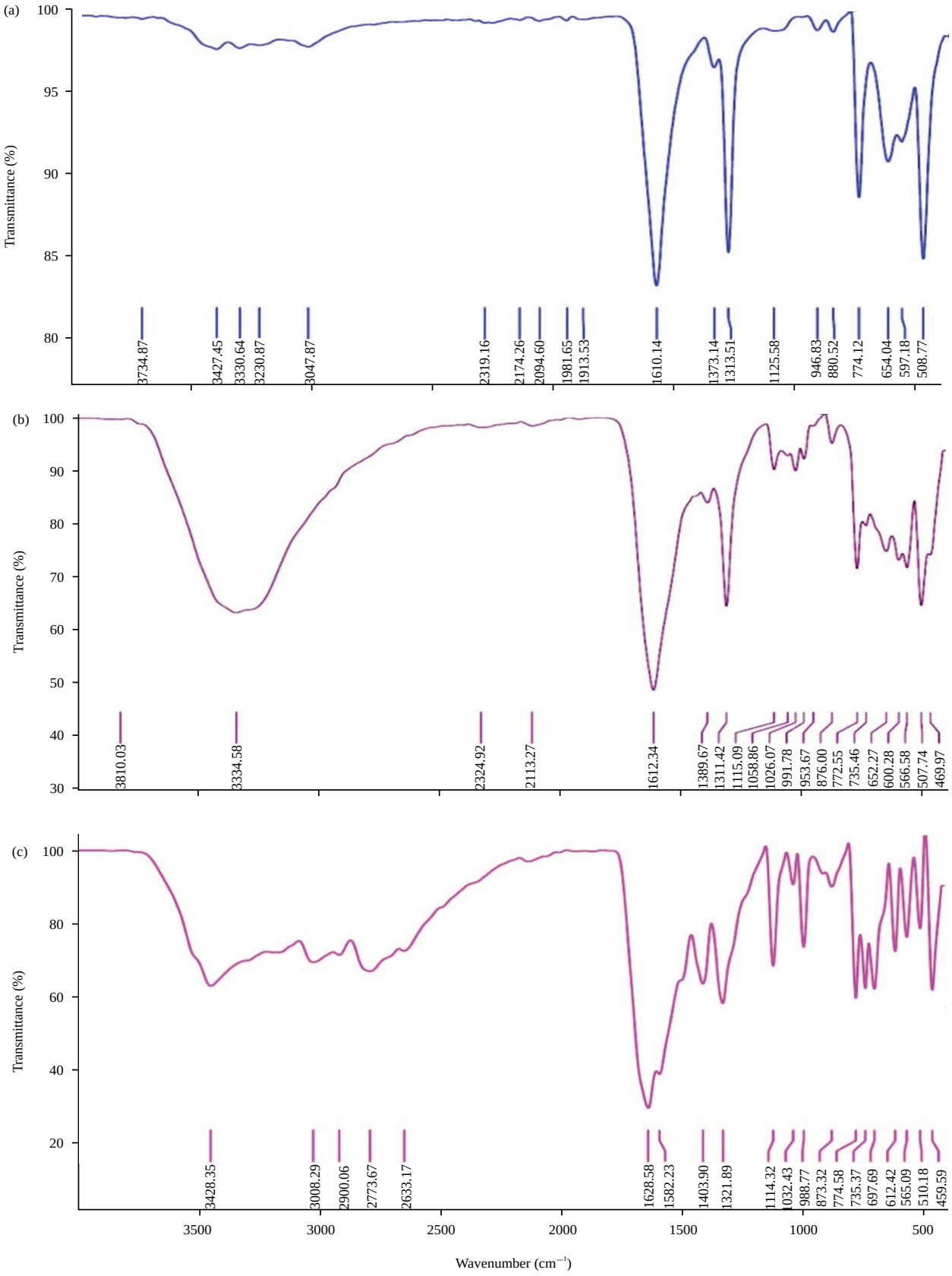

Fig. 1(a-e): Continued

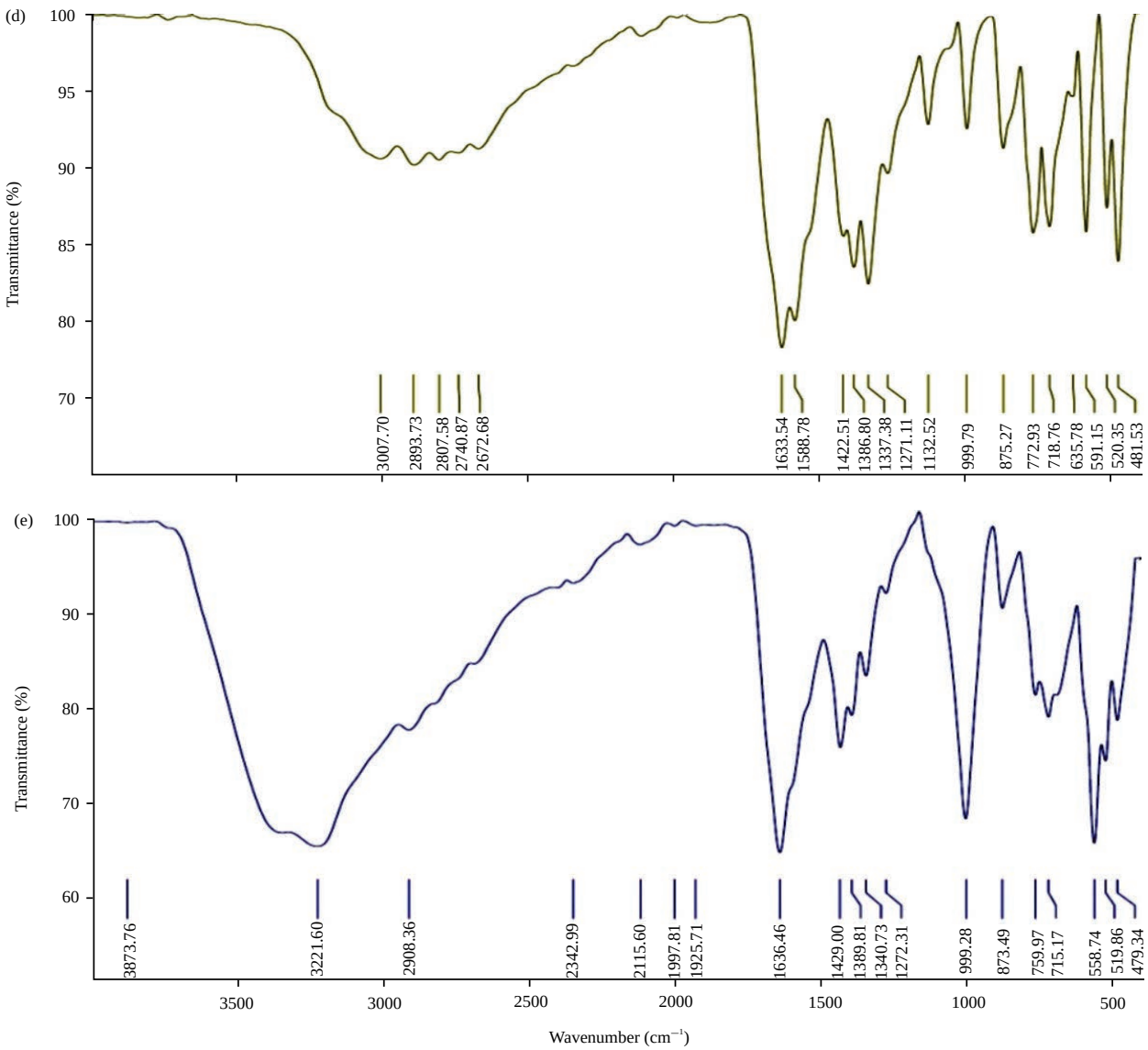

Fig. 1(a-e): FTIR spectrum showing the spectra of different types of stones
(a) COM and CaP, (b) CaP and CaOX, (c) MgAmP, (d) Amu and P and (e) COD and CaP

Isolation and detection of nanobacteria

Detection of nano-bacterial growth by spectrophotometer: Detection of NB was estimated during time intervals using a U.V. spectrophotometer. Results presented in Table 3, revealed that out of 54 kidney stones samples, Total 32 samples (59.26%) were positive for nano-bacterial infection, where Optical Density (OD) measurement increased along the test period (28 days), While 22 samples (40.74%), didn`t show any detectable increase in (OD) indicating that they were negative for nano-bacterial infection.

Macroscopic and Microscopic detection of NB: Macroscopic detection of NB on DMEM medium revealed white growth of dense particles in small groups moving near the bottom of the culture vessel after 1 weak culture period. While, after two weeks, they had become bigger and formed visible groups that penetrated the medium layer. By following the growth after one month, many; were in clumps and attached to the bottom.

All collected stones were investigated by LM with an oil lens (100/1.25) and revealed Gram-ve cocci surrounded by amorphous substances (shells) as shown in Fig. 2a-b.

Urease production test: Results indicated that nano-bacterial isolates were negative for urease activity where it wasn't capable of hydrolyzing urea to produce ammonia and carbon dioxide so the colour of urea slant wasn't changed in comparison to *Proteus* sp. (as positive control).

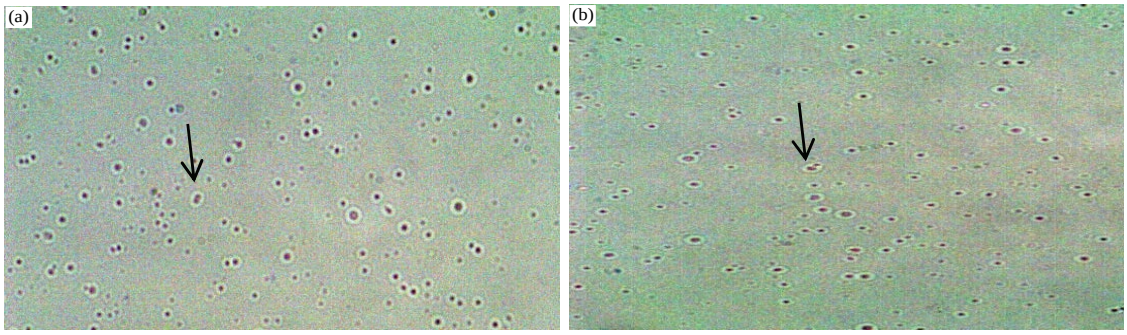

Fig. 2(a-b): Light microscopic detection of nanobacteria
(a) Coccoid nanobes and (b) Nanobes surrounded by shell referred by arrow

Table 3: Detection of nano-bacterial growth by spectrophotometer

Isolate no.	0 day	7 days	14 days	28 days	Isolate no.	0 day	7 days	14 days	28 days
1	0.02	0.25	0.81	1.23	17	0.02	0.29	0.43	0.99
2	0.03	0.12	0.23	0.83	18	0.02	0.31	0.40	0.86
3	0.02	0.17	0.35	0.55	19	0.02	0.28	0.82	1.06
4	0.08	0.18	0.26	0.51	20	0.09	0.18	0.23	0.63
5	0.09	0.12	0.24	0.45	21	0.08	0.13	0.34	0.64
6	0.08	0.17	0.21	0.30	22	0.02	0.32	0.88	1.13
7	0.06	0.20	0.36	0.85	23	0.01	0.31	0.62	0.85
8	0.09	0.38	0.94	1.20	24	0.09	0.29	0.85	0.98
9	0.09	0.15	0.23	0.37	25	0.04	0.18	0.23	0.36
10	0.02	0.27	0.38	0.40	26	0.04	0.10	0.40	0.92
11	0.02	0.23	0.80	1.08	27	0.04	0.11	0.24	0.75
12	0.03	0.21	0.52	0.77	28	0.05	0.10	0.30	0.98
13	0.03	0.21	0.82	1.17	29	0.02	0.09	0.12	0.27
14	0.08	0.18	0.35	0.99	30	0.03	0.13	0.30	0.83
15	0.02	0.25	0.75	098	31	0.07	0.16	0.21	0.80
16	0.02	0.12	0.27	0.78	32	0.09	0.28	0.34	0.97

Detection of NBs by SEM with EDX and TEM

Scanning electron microscope: All the collected kidney stones with positive nano-bacterial infection were subjected to SEM analysis. SE micrographs of 30 days old of the tested culture showed clusters of coccoid nanobes and separated coccal NB (Fig. 3a-b) with magnification power x5 and 7.5 respectively. The size of all the previously mentioned nanobes is in the range from 375-600 nm. Also, the SE micrograph is shown in Fig. 3c-d referred to the bacilliform of nanobacteria and also clearly indicates that the nano-bacterial cell surrounded by a mineral shield (referred by arrows) that protects it from the effect of antimicrobial drugs.

Moreover, Fig. 4a-b Proved the biofilm formation ability of nanobes, which represent a defence mechanism towards the antimicrobial drugs.

Transmission electron microscope: Transmission electron microscope revealed that nano-bacterial isolates have a spherical coccoid shape with thick cell walled structures forming a mineral structure. The cell wall and capsule were distinct and surrounding the organism by hairy apatite structure (Fig. 5a-b). Also, Fig. 6 described TEM of nanobacteria that reproduced by binary fission (Referred by arrows).

Chemical analysis of the NBs shield using Fourier Transforms Infrared Spectroscopy (FTIR)

FTIR: FTIR technique was used to analyze the composition of the nano-bacterial mineralized shell. FTIR spectrum analysis showed an abnormal peak between 1000 and 1200 cm^{-1} which belonged to phosphate absorption and a peak less than 900 cm^{-1} belonging to the stretching bond of phosphate in the hydroxyapatite structure of nanobacteria mineralized shell (Fig. 7).

Energy-dispersive x-ray (EDX) spectra analysis: EDX is an analytical method used for the elemental investigation of the nano-bacterial isolates shield Fig. 8a showed SEM analysis of nano-bacterial isolates, Fig. 8b presented mapping of nanobacteria pellet which exhibited the traditional elements established within the bacterial cell such as K, P, Na, O, N and

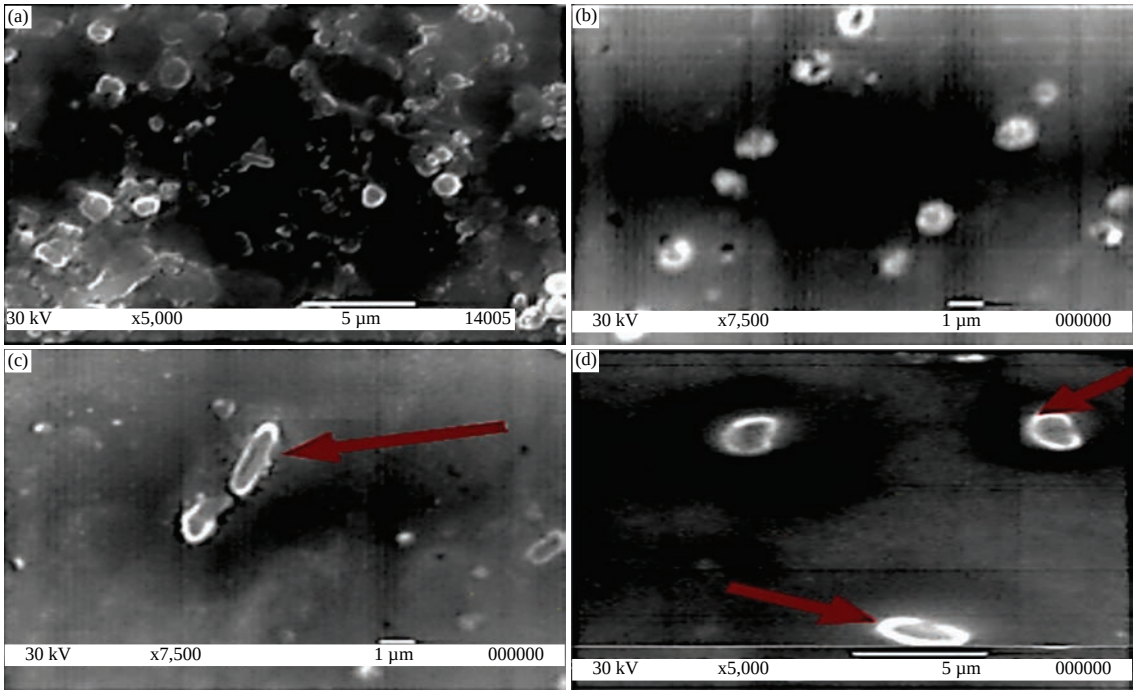

Fig. 3(a-d): SE micrograph of nanobacteria isolates showing
(a-b) Variable shape and size at different magnification power (1-5 µm) and (c-d) NB mineral shield

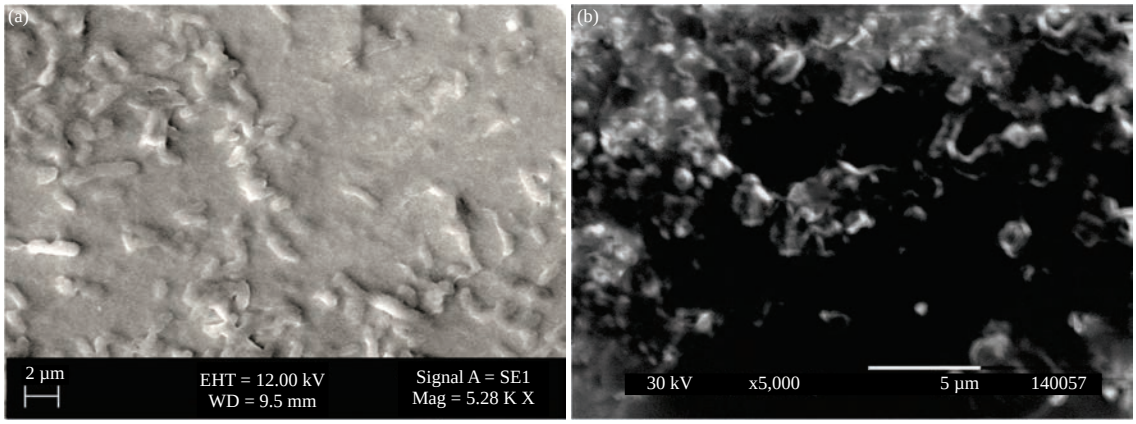

Fig. 4(a-b): SE micrograph showing the biofilm formation of NB
(a) Nanobacteria biofilm formation (bar = 2 µm) and (b) Nanobacteria biofilm formation (bar 5 µm)

C. Figure 8c also showed notable absorption peaks related to nano-bacterial shield as C, 22.41-33.27%; K, 15.25-6.25%; N, 10.57-13.47% and Ca, 3.39-2.44%. While Mg content was 2.22-0.95%. Finally, the Na and P contents were (1.11-0.86%) and (1.05-0.78%), respectively.

Qualitative determination of biofilm production by nano-bacterial isolates: The production of adherent biofilm was equally apparent at the wall and bottom of flasks after 2 weeks. The produced biofilm becomes more visible and tightly attached to the bottom after one month Fig. 9a-c, respectively.

Quantitative determination of biofilm production by nano-bacterial isolates using ELISA method: Biofilms are a survival strategy used by bacteria in natural and industrial systems and in the medical field as a protection against chemical antibacterial substances (including natural antibiotics),

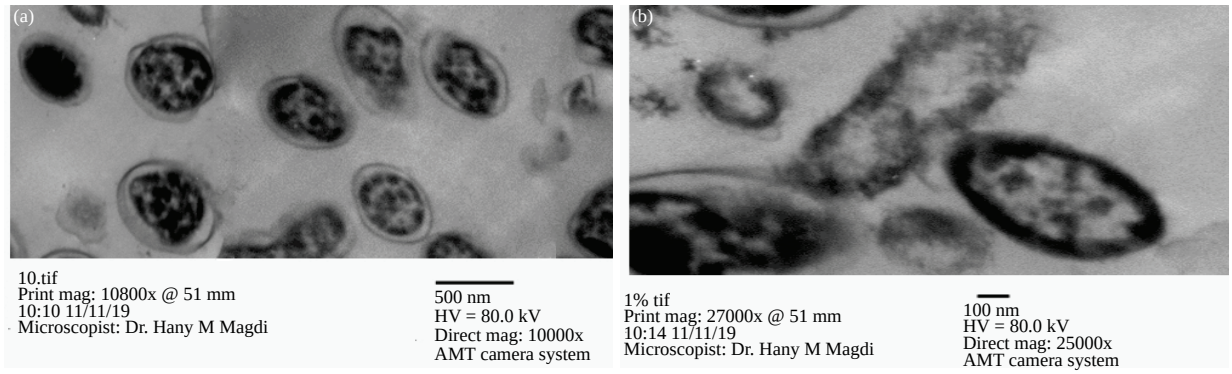

Fig. 5(a-b): Transmission electron micrograph showing of NB at 10000X and 25000X magnification (Bar = 500 nm)
(a) Thick cell walled structure with distinct capsule and (b) Hairy apatite structure

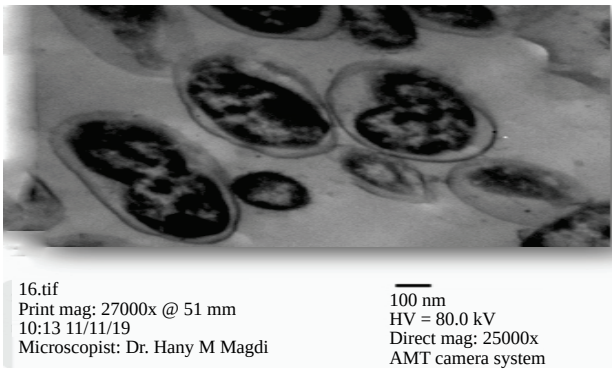

Fig. 6: Transmission electron micrograph showing NB at 25000X magnification (Bar = 500 nm) with apparently binary fission

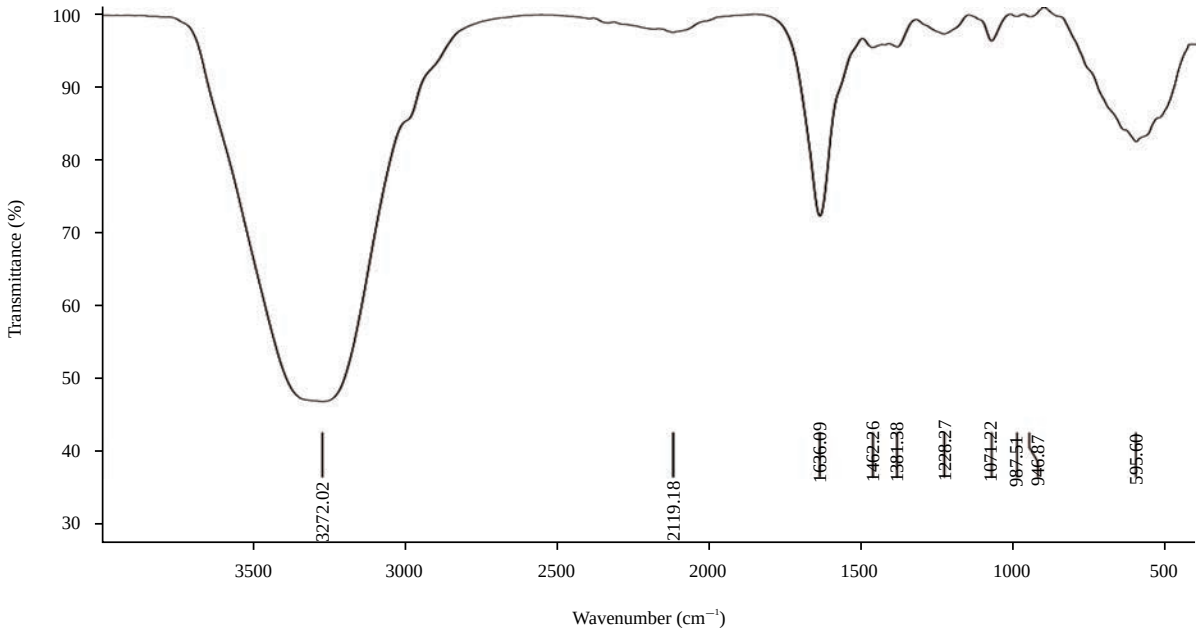

Fig. 7: FTIR spectrum of nano-bacterial isolates

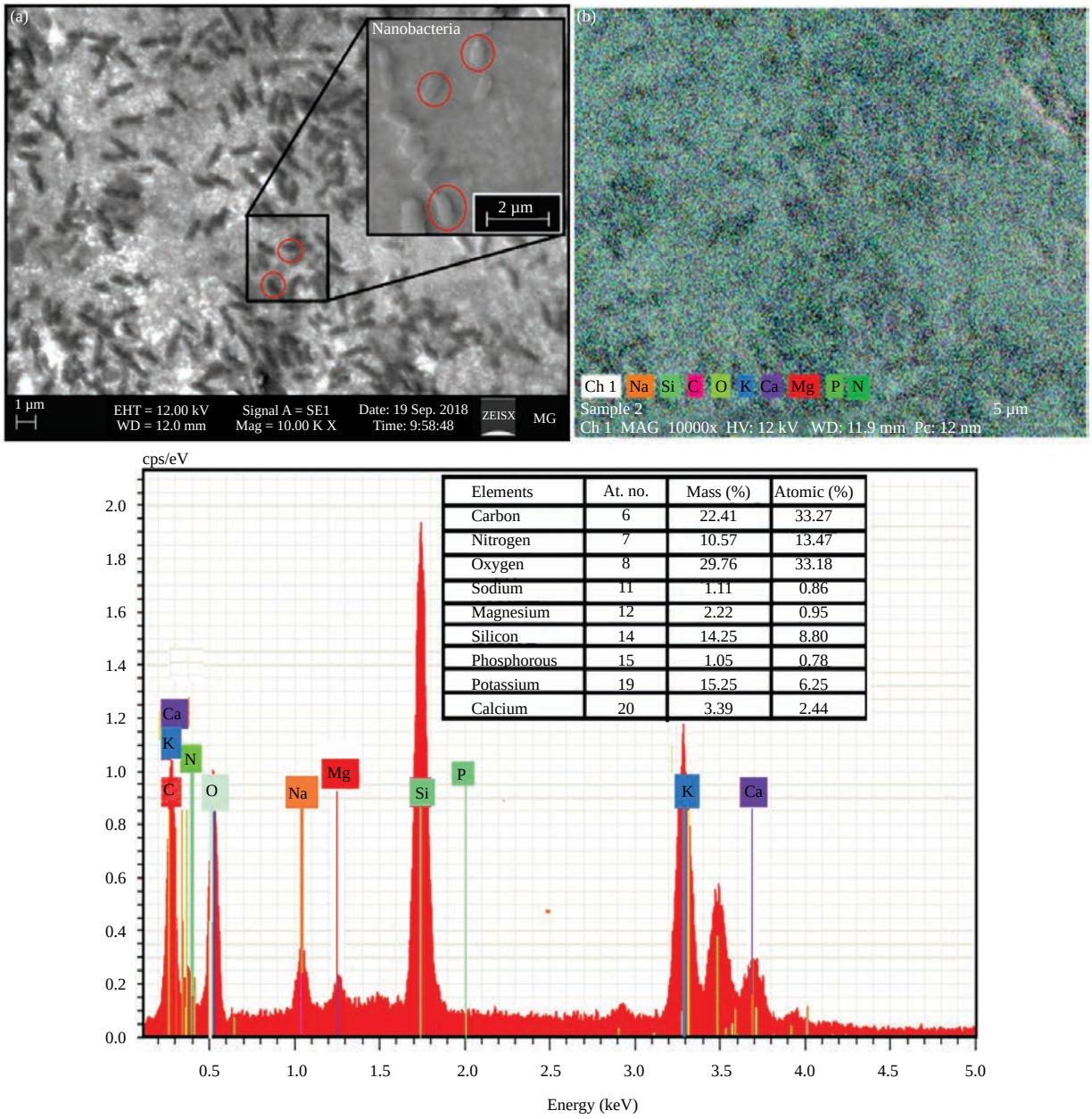

Fig. 8(a-c): Surface morphology and elemental analysis of NB
(a) SEM image, (b) Mapping of NB pellet and (c) EDX elemental analysis of NB pellet

environmental bacteriophages, phagocytic cells and irradiation. Bacteria within a biofilm can be 1,000 times more resistant to antibiotics than their planktonic counterparts.

Biofilm production of nano-bacterial isolates was estimated quantitatively by the ELISA method. It was found that all nano-bacterial isolates were strong biofilm producers with ODs ranged from 0.227-1.372.

Identification of nanobacteria by 16S rRNA and phylogenetic analysis: The most drug-resistant and potent biofilm producer isolate was identified genetically by ribosomal ribonucleic acid (rRNA). Neighbour-Joining phylogeny tree of the output result of BLAST revealed that the submitted gene corresponding to rRNA sequence is indicated by (85.37%) to *Bartonella apis* strain PEB0122. Figure 10. Nanobacteria were submitted in Gene bank as *Nanobacterium* sp. strain BA 1 16S ribosomal RNA gene, the partial sequence with accession number: (MW879444).

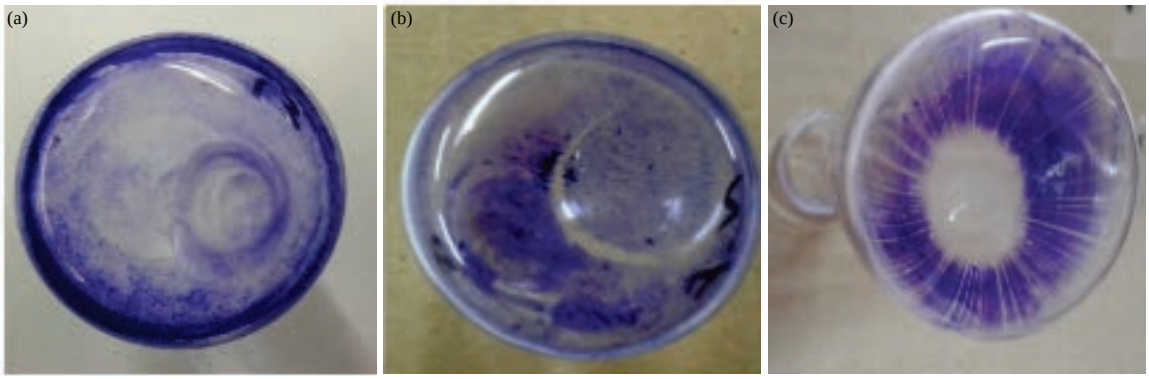

Fig. 9(a-c): Qualitative assay of nano-bacterial isolates for biofilm production
(a) Nano-bacterial biofilm production after 1 weak, (b) Nano-bacterial biofilm production after 2 weak and (c) Nano-bacterial biofilm production after 1 month

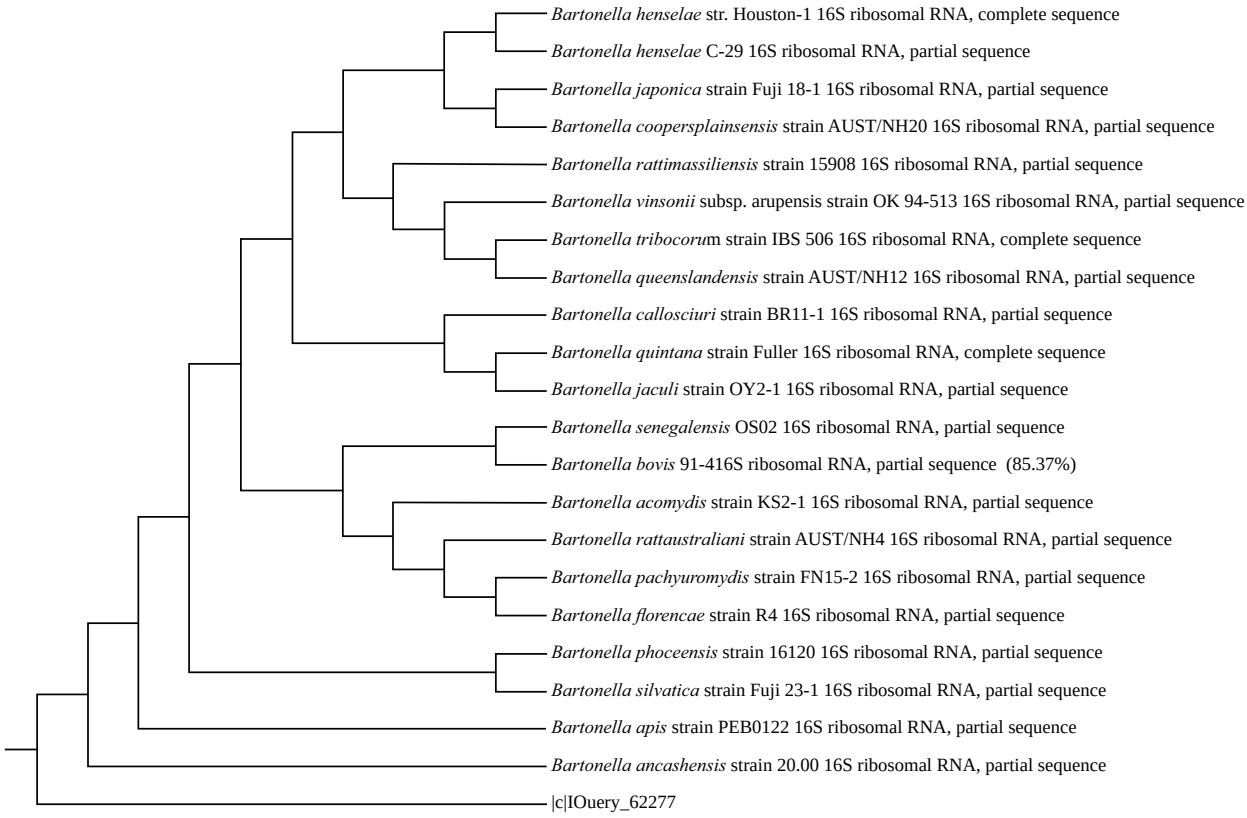

Fig. 10: 16S rRNA alignment reference tree of *Bartonella apis* strain PEB0122 (85.37%)

Antibiotic susceptibility patterns of the strongest nano-bacterial biofilm producers: This investigation was evaluated spectrophotometrically (data were not showed). It was found that streptomycin (S); (SXT) and (DO) have anti-nano-bacterial activity against all isolates but penicillin G., (CIP) and (CEP) haven't any effects.

Microbiological quality of medicinal plants: Medicinal plants are known to be contaminated as a result of harvesting, methods of drying and storage causing a potential hazard to human health. The tested medicinal plants were exposed to increasing doses of gamma radiation from 1-10 kGy. Thyme, khella, neem, fennel and halfa bar showed the highest microbial load among samples.

Table 4: MICs of the selected antibiotics on biofilm production by the strongest nano-bacterial biofilm producers

	MICs of antibiotics (μg mL^{-1})	
Isolate no.	S	Do
47	7.8	3.9
21	7.8	3.9
12	3.9	3.9
10	7.8	7.8

Table 5: MICs of WEs of the selected medicinal plants on biofilm production by the strongest nano-bacterial biofilm producer

	MICs of medicinal plants (WEs) (μg mL^{-1})				
	Khella		Fennel		
Isolate no.	B	F	B	F	Parsley
47	31.2	7.8	62.5	15.6	125
21	62.5	1.9	15.6	15.6	31.2
12	125	1.9	125	62.5	62.5
10	31.2	3.9	15.6	15.6	62.5

Out of the tested plants, thistle, parsley and dill were free from microbial contamination, while, others, thyme, neem and fennel were free from only fungal contamination. Also, it was noticed that δ- irradiation caused a marked decrease in both bacterial and fungal counts and this decrease was proportional with the irradiation dose. The recorded decontamination dose ranged from 5.0-8.0 kGy (Data were not shown).

MIC determination of the selected antibiotics and medicinal plant extracts on biofilm production of the strongest nano-bacterial biofilm producers: The Minimum Inhibitory Concentration (MICs) of the most effective tested antimicrobials on the biofilm formation ability of the strongest biofilm producer isolates were determined. The results indicated that MICs ranged from 7.8-3.9 μg mL^{-1} for both S and DO with a high potentiality of DO on the tested isolate (Table 4).

Water and ethanolic extracts of plants showing high efficacy on the growth of nano-bacterial isolates was chosen for further study to elucidate their efficacy on the biofilm formation ability of the strongest producer isolates. The results presented in Table 5 and 6 showed that MICs of WEs of khella ranged from 125-31.2 μg mL^{-1} before irradiation and from 7.8-1.9 after irradiation at dose level 5 kGy. MICs of fennel were ranged from 125-15.6 μg mL^{-1} and from 62.5-15.6 μg mL^{-1} before and after irradiation at 6 kGy, respectively. While MICs of unirradiated parsley were ranged from 125-31.2 μg mL^{-1}. On the other hand, MICs of EEs of khella were ranged from 31.2-15.6 and from 31.2-7.8 before and after irradiation at dose 5 kGy, respectively. In the case of halfa bar, MICs were ranged from 31.2-15.6 μg mL^{-1} for both irradiated and unirradiated samples at dose level 8 kGy. MICs of thyme were ranged from 62.5-15.6 and from 62.5-7.8 for irradiated and unirradiated thyme at dose 4 kGy, respectively.

Combination treatment between the most potent agents on biofilm production of the strongest nano-bacterial biofilm producers: This study was carried out on the most nano-bacterial biofilm producer isolates to elucidate the synergistic effect of the effective antibiotic (DO) in combination with WE of irradiated khella to identify a system that might be used to improve the efficiency of the anti-nano-bacterial agents used. The results were presented in Table 7.

Data from Table 7 confirmed that DO inhibits the biofilm formation ability of nano-bacterial isolates more than S where there was a highly significant decrease between DO and control, while non-significant difference appeared by using S. It worth noting that combination treatment between DO and khella extract exhibited a synergistic effect on biofilm formation ability. Where isolate no. 21 has a strong ability to produce biofilm (OD = 0.539), by applying DO, it was changed to 0.089, while the combination treatment showed a highly significant decrease for week ability to produce biofilm (OD = 0.059). Also, isolate no. 12 has a strong ability to produce biofilm with OD = 0.312 using DO, significantly reduce its ability to produce biofilm (OD = 0.092), in the case of the combination treatment, there was a significant decrease in its power of adherence to 0.070. Moreover, the power of adherence of isolate no. 10 was 0.422 and when treated with DO, it was 0.106. For combination treatment, there was a significant decrease in the power of adherence to 0.068.

These findings will encourage efforts toward the development of novel anti-nano-bacterial agents that could be better in terms of efficacy and safety.

DISCUSSION

Nanobacteria were recognized in human kidney stones for the first time where NB are very tiny agents, which are 100-fold smaller than common bacteria. They are sheltered by a crystalline carbonate apatite shell membrane. In this study, males were at higher risk of infection than females and these results were following Shojaiyan *et al.*[24] who found that male patients are significantly prone to kidney stone formation in comparison with females, 70 and 30%, respectively. Also,

Table 6: MICs of EEs of the selected medicinal plants on biofilm production by the strongest nano-bacterial biofilm producer

	MICs of medicinal plants (EEs) (μg mL^{-1})					
	Khella		Halfa bar		Thyme	
Isolate no.	B	F	B	F	B	F
47	31.2	7.8	15.6	31.2	62.5	62.5
21	31.2	31.2	15.6	15.6	15.6	15.6
12	31.2	15.6	31.2	31.2	62.5	15.6
10	15.6	15.6	15.6	15.6	31.2	7.8

Table 7: Combination treatment between antibiotics, WE of irradiated khella at their MICs on the biofilm production by the strongest nano-bacterial biofilm producers

	Power of adherence					
	Treated				Combination treatment	
Isolate no.	Control	Do	S	Khella (WE)	Do+Khella (WE)	S+Khella (WE)
47	0.475±0.005	0.063±0.002[a]	0.071±0.001[b]	0.119±0.006[a]	0.061±0.002[a]	0.063±0.002[b]
21	0.539±0.029	0.089±0.002[a]	0.100±0.001[b]	0.137±0.006[a]	0.059±0.001[a]	0.152±0.002[b]
12	0.312±0.013	0.092±0.003[a]	0.072±0.003[b]	0.126±0.003[a]	0.070±0.003[a]	0.082±0.004[b]
10	0.422±0.015	0.106±0.005[a]	0.058±0.002[b]	0.180±0.002[a]	0.082±0.003[a]	0.068±0.005[b]

Data represented as mean±SEM. [a]Significantly different from control at $p \leq 0.05$, [b]Non-significant different from control at $p \leq 0.05$

Scales[25] found that the prevalence of stones was 10.6% among men, compared with 7.1% among women. Freeg *et al.*[26] found that the male to female ratio was 5:1 where 87% of the patients were aged thirty to sixty years and 11 patients were under age fourteen out of 760 Saudi patients with urolithiasis. The chemical analysis of the examined stones indicated that the most main types of stones were COM and CaP (44.44%), followed by CaP and CaOX (24.07%), while Mg AmP, AmU and P and COD and CaP were 22.22, 5.56 and 3.71%, respectively. Several studies conducted by many authors[24,27,26] found that the most prevalence of stones belongs to calcium oxalate while, Emam *et al.*[1] found that 50% of the collected stones were identified as urates, 30% as oxalates and 20% as phosphates.

Simonetti *et al.*[28] analyzed the stones by EDX and indicated that the stones consisted mainly of calcium with the presence of phosphate. They also concluded the presence of carbon, even in low concentrations. Generally, calcium oxalate is the main renal stone component according to the literature.

The presence of nanobacteria was found in 32 samples (59.26%) where similar results were obtained by Emam *et al.*[1] who found that eight out of ten (80%) urinary tract stones showed growth of nanobacteria. A pale white biofilm attached to the bottom of the culture flask was observed in 4 weeks old culture, while the control did not show any growth. Also, Simonetti *et al.*[28] reported that eleven out 27 (41%) kidney stone cultures were positive after eight-week incubation at 37°C, then the NB gradually increased with white-coloured sediment on the bottom of the tubes whereas the control did not show any growth.

Zhang *et al.*[29] showed that after 3-6 weeks of culture, the 11 bladder tissues and six urine samples with the pure growth of NB had white granular sediments firmly attached to the bottom of the culture flasks and these were visible to the naked eye.

The results of the current study were also in agreement with Khullar *et al.*[30] who observed that forty out of 65 tested kidney stones (62%) produced a pale white biofilm attached to the bottom of the culture flask after 4 weeks of incubation, whereas the control did not show any growth.

Scanning electron analysis of white-colour sediments nanobacteria revealed that its size was ranged from 375-600 nm. While, TEM micrograph detected nanobacteria with spherical coccoid shape, thick cell walled structures and cell wall was surrounded by hairy apatite structure. Our results were in agreement with Emam *et al.*[1] who found that the isolated bacteria from urinary tract stones were apatite forming ultra-filterable self-replicating coccoid microorganisms of a diameter ranging from 100-600 nm which shows variable-sized nanobacteria with a distinct cell wall and capsule. Another study conducted by Wang *et al.*[31] showed that NB ranged from 80-500 nm and appeared gathered in the form of coccobacillus. Some of them were partially or completely covered with a thick or thin layer of hydroxyapatite.

Also, results were similar to that obtained by Ansari *et al.*[32] where TEM indicate various sizes of nanobacteria with a hairy appearance, which is a discriminating feature of the nanobacteria. Also, the results obtained by other authors

Emam *et al.*[1] and Khullar *et al.*[30] showed that NB was coccoid with thick cell walled structures. Cell wall and surrounded by hairy apatite.

The results from FTIR and EDX confirmed that NB has calcium and phosphate as main constituents. The results were agreed with that obtained by Ansari *et al.*[32] which revealed that the main components of the shell were hydroxyapatite and calcium apatite. These apatite complexes did not exist in the kidney stones of the patients that were not infected by nanobacteria. These results confirmed the bio-mineralization activity of NB and the obtained results with Sardarabadi *et al.*[33-,34] who found that EDX analysis of NB in the culture medium showed calcium and phosphate peaks rather than other minerals such as magnesium and sodium.

The result was indicated that according to the submitted gene corresponding to rRNA sequence, nanobacteria was identified (85.37%) to *Bartonella apis* strain *PEB0122* and this result was compatible with Breitschwerdt *et al.*[35] who detected the nano-bacterial antigen in North Carolina cattle which had a 16srRNA sequence identical to *Bartonella* sp.

Hjelle *et al.*[36] found that around 10 liver cyst fluids were positive for nanobacteria and were also positive for Bartonella that through dot-immunoblot analysis for samples. Also, there were 21 kidney cyst fluids that were positive for both Bartonella and nanobacteria while one was weakly positive only for nanobacteria and two were weakly positive only for Bartonella. Based on the respective 16S rRNA sequences, Bartonella and Nano bacterium spp. are members of the α2 subgroup of Proteobacteria.

Antibiotic susceptibility towards the strongest nano-bacterial biofilm producer was found that S, SXT and DO have anti-nano-bacterial activity against all isolates. The results were similar to that obtained by Abo-El-Sooud *et al.*[37] and Ciftcioglu *et al.*[9] who found that NB was inhibited *in vitro* at clinically achievable levels in serum and urine by ampicillin, trimethoprim, trimethoprim-sulfamethoxazole, nitrofurantoin (a urinary antiseptic) and tetracycline HCl. While, Drancourt *et al.*[38] found that NB was resistant to most antibiotics. So, there are calls for novel pharmacological therapeutical and preventive measures. One approach to tackle this issue is to explore the therapeutic properties of medicinal plant extracts. thistle, parsley, khella, dill, thyme, halfa bar, neem and fennel are considered the oldest documented medicinal plants that have been used for centuries in traditional Arabic medicine for the treatment of kidney stones.

Ciftcioglu *et al.*[9] suggested that the *in vitro* activity of doxycycline against NB (MIC, 62.5 μg mL^{-1}) may be due to its high protein-bound and approximately 10 times more lipophilic than tetracycline HCl (MIC, 1.95 μg mL^{-1}). Where their activities against NB observed in vitro were correlated with their comparative levels of calcium-binding. While, the aminoglycosides were primarily known as inhibitors of protein synthesis, but more recently it has been recognized that they displace cell biofilm-associated calcium and magnesium that link polysaccharides of lipopolysaccharide molecules.

A study conducted by Aljanaby[39] demonstrated that both cold-water and hot-water extracts of parsley leaves had inhibitory activity against *P. aeruginosa*, *S. aureus* and *S. pyogenes,* with the hot water extract at 250 mg mL^{-1} resulting in the largest inhibition zones. A similar study conducted by Kaur and Arora[40] recorded MIC 60 mg mL^{-1} of aqueous extract of fennel against *E. coli* and *S. aureus*. Jaradat *et al.*[41] reported that aqueous extracts of khella possessed antibacterial activity with MIC = 25 mg mL^{-1} against both G +ve *Staph. aureus* and G-ve *E. coli* and *P. aeruginosa*. Generally, the results of the current study revealed that water extracts of irradiated samples seem to be most effective than unirradiated or ethanolic ones, therefore, water extracts of irradiated samples were chosen for further studies.

Zantar *et al.*[42] documented that gamma irradiation at dose levels 10, 20 and 30 kGy affected quantitatively and not qualitatively some components of the dried leaves and flowers of thyme oil. This effect was dose-dependent. The antimicrobial activity increased in the irradiated samples for Gram-negative bacteria and did not change for Gram-positive bacteria, while the antioxidant activity remains stable at any dose applied for the plants studied.

Our results are following that reported by Atef *et al.*[43] where they reported that water and methanolic extracts of *Moringa oleifera* L. (leaves) and *Matricaria recutita* L. (flowers) represented good activity against the tested isolates whereas ethanolic extract of both plants showed a lesser activity. In contrary to our results, Sabry *et al.*[44] revealed that the organic extracts of Halfa-bar were more effective than the aqueous extract and showed high antibacterial activity against all the tested pathogenic bacteria.

It is a promising study for combination treatment between doxycycline and water extract of irradiated khella at 5 kGy dose level for inhibiting drug-resistant biofilm producer nanobacteria. Further study could be carried out in near future on lab animal (*in vivo* testing) to confirm the efficiency of irradiated khella as an anti-nano-bacterial agent with safety application in the medical field.

CONCLUSION

The results of this study demonstrated the strong ability of NB to produce drug-resistant biofilms. For this reason, there is an urgent need to discover new anti-nano-bacterial agents that can inhibit biofilm formation. This current study showed encouraging data for antibiofilm efficacy when combination treatment is applied between convenient antibiotic (DO) and water extract of irradiated khella which is considered as a promising protocol for managing dangerous infections especially those caused by NB.

SIGNIFICANCE STATEMENT

This study discovers the antibiofilm efficiency of combination treatment between antibiotic (DO) and water extract of irradiated khella that can be beneficial for inhibiting biofilm formation and development of nanobacteria which causing kidney stones. This study will help the researcher to uncover the critical areas of kidney stone formation that many researchers were not able to explore. Thus a new theory on combination treatment between antibiotic and natural product may be arrived at.

ACKNOWLEDGMENT

Our sincere thanks extend to central labs of NCCRT (Egyptian atomic energy authority) for their sincere cooperation.

REFERENCES

1. Emam, M., N.A. Ezzeldeen, M.M. Hashem and A. Ramadan, 2014. Phenotypic characterization of *Nanobacterium* sp. isolated from urinary tract calculi of Egyptian patients. Intl. J., 5: 98-104.
2. Kutikhin, A.G., E.B. Brusina and A.E. Yuzhalin, 2012. The role of calcifying nanoparticles in biology and medicine. Int. J. Nanomed., 7: 339-350.
3. Zhang, M.J., S.N. Liu, G. Xu, Y.N. Guo, J.N. Fu and D.C. Zhang, 2014. Cytotoxicity and apoptosis induced by nanobacteria in human breast cancer cells. Int. J. Nanomed., 9: 265-271.
4. Yaghobee, S., M. Bayani, N. Samiei and N. Jahedmanesh, 2015. What are the nanobacteria? Biotechnol. Biotechnol. Equip., 29: 826-833.
5. Kumar, C.A., M. Bagga, V. Mohan and N. Raghav, 2011. An overview on clinical implications of nanobacteria. J. Indian Acad. Oral Med. Radiol., 23: S354-S359.
6. Kajander, E.O., N. Ciftcioglu, K. Aho and E. Garcia-Cuerpo, 2003. Characteristics of nanobacteria and their possible role in stone formation. Urol. Res., 31: 47-54.
7. Ramalingam, S.R., P. Sarkaraisamy and P. Seeni, 2014. *In-vitro* effect of cystone against calcifying microorganism isolated from human kidney stone. Int. J. Pharm. Sci. Res., 5: 3952-3956.
8. Adedapo, A.A., F.O. Jimoh, S. Koduru, A.J. Afolayan and P.J. Masika, 2008. Antibacterial and antioxidant properties of the methanol extracts of the leaves and stems of *Calpurnia aurea*. BMC Complement. Altern. Med., Vol. 8, No. 1. 10.1186/1472-6882-8-53.
9. Ciftcioglu, N., M.A. Miller-Hjelle, J.T. Hjelle and E.O. Kajander, 2002. Inhibition of nanobacteria by antimicrobial drugs as measured by a modified microdilution method. Antimicrob. Agents Chemother., 46: 2077-2086.
10. Christensen, W.B., 1946. Urea decomposition as a means of differentiating proteus and paracolon cultures from each other and from *Salmonella* and shigella types. J. Bacteriol., 52: 461-466.
11. Simonetti, A.B., G.E. Englert, K. Campos, M. Mergener, C. de David, A.P. de Oliveira and P.M. Roehe, 2007. Nanobacteria-like particles: A threat to cell cultures. Braz. J. Microbiol., 38: 153-158.
12. Bozzola, J.J. and L.D. Russell, 1999. Electron Microscopy: Principles and Techniques for Biologists. 1st Edn., Jones and Bartlett Publishers International, London, ISBN-13: 978-0867201260, Pages: 542.
13. Christensen, G.D., W.A. Simpson, A.L. Bisno and E.H. Beachey, 1982. Adherence of slime-producing strains of *Staphylococcus epidermidis* to smooth surfaces. Infec. Immun., 37: 318-326.
14. Christensen, G.D., W.A. Simpson, J.J. Younger, L.M. Baddour, F.F. Barrett, D.M. Melton and E.H. Beachey, 1985. Adherence of coagulase-negative staphylococci to plastic tissue culture plates: A quantitative model for the adherence of staphylococci to medical devices. J. Clin. Microbiol., 22: 996-1006.
15. Baldassarri, L., W.A. Simpson, G. Donelli and G.D. Christensen, 1993. Variable fixation of staphylococcal slime by different histochemical fixatives. Eur. J. Clin. Microbiol. Infect. Dis., 12: 866-868.
16. Vasanthi, R., D. Karthikeyan and M. Jeya, 2014. Study of biofilm production and antimicrobial resistance pattern of the bacterial isolates from invasive devices. Int. J. Res. Health Sci., 31: 274-281.
17. NCCLS., 2018. Methods for Dilution Antimicrobial Susceptibility Tests for Bacteria that Grow Aerobically. 11th Edn., National Committee for Clinical Laboratory Standards, United States, ISBN-10: 1-56238-836-3, Pages: 91.

18. Hannan, P.C., G.D. Windsor, A. de Jong, N. Schmeer and M. Stegemann, 1997. Comparative susceptibilities of various animal-pathogenic mycoplasmas to fluoroquinolones. Antimicrob. Agents Chemother., 41: 2037-2040.
19. ICMSF., 1986. Microorganisms in Foods. Sampling for Microbiological Analysis: Principles and Specific Applications. 2nd Edn., Blackwell Scientific Publications, United States, Pages: 198.
20. Koburger, J.A. and E.H. Marth, 1984. Yeasts and Molds. In: Compendium of Methods for the Microbiological Examination of Foods, Speck, M.L. (Ed.)., American Public Health Association, Washington DC, pp: 197-201.
21. Charchafchi, F.A., I. Al-Nabhani, H. Al-Kharousi, F. Al-Quraini and A. Al-Hanai, 2007. Effect of aqueous extract of *Azadirachta indica* (neem) leaves on germination and seedling growth of *Vigna radiata* (L.). Pak. J. Biol. Sci., 10: 3885-3889.
22. Najmadeen, H.H. and F.K. Kakamand, 2009. Antimicrobial activity of propolis collected in different regions of Sulaimani province-Kurdistan region/Iraq. J. Duhok Univ., 12: 233-239.
23. Milton, J.S., J.J. Corbert and P.M. McTeer, 1986. Introduction to Statistics. 3rd Edn., McGraw-Hill Companies, Canada, Toronto, ISBN-13: 978-0071145237, Pages: 736.
24. Shojaeian, A., M. Rostamian, J. Noroozi and P. Pakzad, 2016. The identification of chemical and bacterial composition and determination of FimH gene frequency of kidney stones of Iranian patients. Zahedan J. Res. Med. Sci., Vol. 18. 10.17795/zjrms-7363.
25. Scales Jr, C.D., A.C. Smith, J.M. Hanley and C.S. Saigal, 2012. Prevalence of kidney stones in the United States. Eur. Urol., 62: 160-165.
26. Freeg, M.A.H.A., J. Sreedharan, J. Muttappallymyalil, M. Venkatramana, I.A. Shaafie and E. Mathew *et al*., 2012. A retrospective study of the seasonal pattern of urolithiasis. Saudi J. Kidney Dis. Transpl., 23: 1232-1237.
27. Abdelarheim, G. and M.S. Al-Aboodi, 2013. Attempts for detection of nanoparticles-nanobacteria and distribution of their antibodies in saudi patients with urolithiasis. Eur. Sci. J., 9: 97-106.
28. Simonetti, A.B., C.T.D. Ros, C. de David, K. Campos, P.R.P. Behar, E. Ribeiro and G.E.N. Hidalgo, 2012. Occurrence of nanobacteria-like particles in renal stones of a southern Brazilian population. Open J. Urol., Vol. 2. 10.4236/oju.2012.21001.
29. Zhang, Q.H., X.C. Shen, Z.S. Zhou, Z.W. Chen, G.S. Lu and B. Song, 2010. Decreased nanobacteria levels and symptoms of nanobacteria-associated interstitial cystitis/painfuL bladder syndrome after tetracycline treatment. Int. Urogynecol. J., 21: 103-109.
30. Khullar, M., S.K. Sharma, S.K. Singh, P. Bajwa, F.A. Sheikh, V. Relan and M. Sharma, 2004. Morphological and immunological characteristics of nanobacteria from human renal stones of a north Indian population. Urol. Res., 32: 190-195.
31. Wang, L., W. Shen, J. Wen, X. An, L. Cao and B. Wang, 2006. An animal model of black pigment gallstones caused by nanobacteria. Digestive Dis. Sci., 51: 1126-1132.
32. Ansari, H., A.A. Sepahi and M.A. Sepahi, 2017. Different approaches to detect "nanobacteria" in patients with kidney stones: An infectious cause or a subset of life? Urol. J., 14: 5001-5007.
33. Sardarabadi, H., M. Mashreghi, K. Jamialahmadi, M.M. Matin and M. Darroudi, 2019. Selenium nanoparticle as a bright promising anti-nanobacterial agent. Microb. Pathog., 126: 6-13.
34. Sardarabadi, H., M. Mashreghi, K. Jamialahmadi and T. Dianat, 2014. Resistance of nanobacteria isolated from urinary and kidney stones to broad-spectrum antibiotics. Iran J. Microbiol., 6: 230-233.
35. Breitschwerdt, E.B., S. Sontakke, A. Cannedy, S.I. Hancock and J.M. Bradley, 2001. Infection with *Bartonella weissii* and detection of nanobacterium antigens in a north carolina beef herd. J. Clin. Microbiol., 39: 879-882.
36. Hjelle, J.T., M.A. Miller-Hjelle, I.R. Poxton, E.O. Kajander and N. Ciftcioglu *et al*., 2000. Endotoxin and nanobacteria in polycystic kidney disease. Kidney Int., 57: 2360-2374.
37. Abo-El-Sooud, K., M.M. Hashem and A.Q. Gab-Allaha, 2012. *In vitro* assessment of different antibacterials against nanobacteria isolated from kidney stones. Insight Nanotechnol., 2: 1-6.
38. Drancourt, M., P. Berger and D. Raoult, 2004. Systematic 16S rRNA gene sequencing of atypical clinical isolates identified 27 new bacterial species associated with humans. J. Clin. Microbiol., 42: 2197-2202.
39. Aljanaby, A.A.J., 2013. Antibacterial activity of an aqueous extract of *Petroselinum crispum* leaves against pathogenic bacteria isolated from patients with burns infections in Al-Najaf governorate, Iraq. Res. Chem. Intermed., 39: 3709-3714.
40. Kaur, G.J. and D.S. Arora, 2009. Antibacterial and phytochemical screening of *Anethum graveolens*, *Foeniculum vulgare* and *Trachyspermum ammi*. Altern. Med., 9: 30-39.
41. Amin, J.N., A. Murad, A.M. Motasem, S.R. Ibrahem, J.M. Ass'ad and A.M. Ayed, 2015. Phytochemical screening and *in-vitro* evaluation of antioxidant and antimicrobial activities of the entire khella plant (*Ammi visnaga* L.) a member of palestinian flora. Int. J. Pharmacogn. Phytochem. Res., 7: 137-143.

42. Zantar, S., R. Haouzi, M. Chabbi, A. Laglaoui and M. Mouhib *et al*., 2015. Effect of gamma irradiation on chemical composition, antimicrobial and antioxidant activities of *Thymus vulgaris* and *Mentha pulegium* essential oils. Radiat. Phys. Chem., 115: 6-11.
43. Atef, N.M., S.M. Shanab, S.I. Negm and Y.A. Abbas, 2019. Evaluation of antimicrobial activity of some plant extracts against antibiotic susceptible and resistant bacterial strains causing wound infection. Bull. Nat. Res. Cent., Vol. 43. 10.1186/s42269-019-0184-9.
44. Sabry, A., S.A. El-Zayat, A.H.M. El-Said, F.F. Abdel-Motaal and T.A. Magraby, 2014. Mycoflora associated with halfa-bar leaves and stems (*Cymbopogon schoenanthus* L. sprengel), *in vitro* the antimicrobial activity of the plant leaves and stems secondary metabolites. Int. J. Curr. Microbiol. Appl. Sci., 3: 874-882.